International Journal of Nanomedicine

Dovepress
open access to scientific and medical research

Open Access Full Text Article

ORIGINAL RESEARCH

An investigation on the cytotoxicity and caspase-mediated apoptotic effect of biologically synthesized gold nanoparticles using *Cardiospermum halicacabum* on AGS gastric carcinoma cells

This article was published in the following Dove Medical Press journal:
International Journal of Nanomedicine

Chunfeng Li[1]
Yimin Wang[1]
Hongfeng Zhang[1]
Man Li[2]
Ziyu Zhu[1]
Yingwei Xue[1]

[1]Gastrointestinal Surgical Ward, Harbin Medical University Cancer Hospital, Harbin, Heilongjiang 150081, China; [2]Department of Endoscopy, Harbin Medical University Cancer Hospital, Harbin, Heilongjiang 150081, China

Background: Gastric cancer is the fourth most common cancer and second leading cause of cancer death worldwide. *Cardiospermum halicacabum* is used to treat nerve disorders, stiffness, rheumatism, ear ache, snake bite, and so on.

Methods: In this study, the reaction parameters were optimized to control the size of the nanoparticle, which was confirmed by transmission electron microscopy. Various characterization techniques such as selected area diffraction pattern, UV-visible spectroscopy, energy-dispersive X-ray analysis, dynamic light scattering, Fourier-transform infrared spectroscopy, and atomic force microscopy were employed to analyze the synthesized AuNPs obtained from *C. halicacabum* (CH-AuNP) against gastric carcinoma cell line.

Results: The cytotoxic effect of CH-AuNP against AGS, SNU-5, and SNU-16 cell lines was detected by MTT assay. The induction of apoptosis by CH-AuNP in AGS was analyzed by double staining technique using TUNEL and DAPI staining assays. Further to confirm the molecular mechanism exhibited by CH-AuNP to induce apoptosis, the intracellular ROS level was assessed and immunoblotting was performed to assess the apoptotic signaling molecules that often deregulated in cancerous condition.

Conclusion: The results clearly prove that CH-AuNP increases ROS and induces apoptosis in AGS, suggesting that CH-AuNP may be an effective anticancer drug with no side effects to treat gastric cancer.

Keywords: gastric cancer, gold nanoparticle *Cardiospermum halicacabum*, apoptosis, MMP, ROS

Introduction

One of the fourth most common and second foremost causes of cancer mortality is gastric cancer.[1] Globocan on the year 2012 estimated that about one million new patients were detected with stomach cancer.[2] About 70% of gastric cancer prevalence was prognosed in developing countries like those in Eastern part of Asia, Europe, and Southern parts of America, and they were affected much more than the rest of the world. The risk of developing gastric cancer was considerably increased to 0.9% in USA. Various risk factors are associated with gastric cancer induction like infection with *Helicobacter pylori*, high alcohol consumption, tobacco smoking, lack of fruit and vegetable intake, more salt consumption in diet, and pernicious anemia.[3]

Among gastric tumor, gastric adenocarcinoma is the common type of cancer that develops from the gastric epithelium. Thirty-four percent of gastric cancer patients

Correspondence: Yingwei Xue
Gastrointestinal Surgical Ward, Harbin Medical University Cancer Hospital, Harbin, Heilongjiang 150081, China
Email xueyingwei_1234@sina.com

submit your manuscript | www.dovepress.com
Dovepress
http://dx.doi.org/10.2147/IJN.S193064

were prone to distant metastasis;[4] hence, chemotherapy seems to be the first choice of treatment in gastric cancer patients.[5] For the advanced stage of gastric cancer, there are numerous multidisciplinary treatment applied to improve the prognosis of patients. The 5-year overall survival rate of patients with advanced gastric cancer is ~25% due to frequent relapse, metastasis, and drug resistance. Thus, further investigations for critical mechanisms on gastric cancer metastasis, relapse, and drug resistance are imperative.[6]

Chemotherapeutic drugs have been used to mimic the tumor cell proliferation through induction apoptosis pathway and the clinic has used these types of drugs today. However, some significant limitations have been shown on their use. Even though there are so many recent advances in chemotherapeutics like introducing inhibitors for immunity checkpoints and targeted drug delivery, the response rate of gastric cancer patients is low.[7] Hence, an effective treatment that prolongs the survival rate and also prevents metastasis is the need of today.

Phytomedicine is an effective treatment done in most of the developing countries, which plays a dramatic role in treating various ailments. China is one such country gifted with tremendous amount of varied medicinal plants that are now considered as weeds. *Cardiospermum halicacabum* is one such plant vernacularly known as balloon plant or love in a puff plant, and it is consumed in the rural south India.[8] *C. halicacabum* was used to treat snake bite, ear ache, diarrhea, dysentery, and emetic, diaphoretic, and nervous disorders.[9–11] The aqueous and ethanolic extracts of *C. halicacabum* possess antiviral, antimicrobial, and antitumor properties.[12] Mass decline in the herbal medicinal plant treatment was noted in the developing countries due to the usage of pure chemical bioactive component in spite of crude drugs; therefore, in the present study, we analyzed the anticancer effect of gold nanoparticles synthesized by *C. halicacabum*.

Gold is a miracle compound that is used to treat various ailments from the ancient days,[13] and recently the gold nanoparticles are used to increase the pharmacokinetics of the existing drug and to reduce the side effect by targeted delivery system.[14] Compared to other metals like silver, the foremost nonreactive property of gold with biologic substance made them to be an appropriate carrier for drugs.[15] It localized surface plasmon resonance, rendering a sturdy optical property and hence improving the drug delivery.[16] Synthesis of gold nanoparticles using plant extracts has been used for the researches based on the stability, a very simple procedure that can be used for the treatment of cancer, gene sequencing, and targeted drug delivery systems. Another advantage of gold nanoparticles is easy bonding between the specific targeted site and anticancer drugs.[17] Because of the several advantages of gold nanoparticles, they have been shown to be used for clinical applications in drug delivery systems and treatment of several types of cancers.

Hence, the present study is aimed to biosynthesize and characterize gold nanoparticles with the herbal plant *C. halicacabum* and to analyze the anticancer property of the synthesized *C. halicacabum* gold particles against gastric adenocarcinoma cell lines.

Materials and methods

Gold(III) chloride trihydrate (99.9%), RPMI 1640 medium, FBS, trypsin, antibiotic solutions, dimethyl sulfoxide, and MTT were purchased from Sigma Aldrich (St Louis, MO, USA).

Sample preparation

Fresh *C. halicacabum* leaves were collected and authenticated. The sample was prepared by thoroughly washing the leaves with sterile distilled water and drying it under the shade till the leaves got dried completely; approximately it took 15 days for drying. The dried leaves were then powdered using an electrical grinder at a minimum speed to avoid heat generation. Fifty grams of finely powdered leaves were mixed with 500 mL of distilled water and boiled for 30 minutes at a temperature of 60°C. The boiled solution was then filtered using Whatmann filter paper and stored at 4°C for the further processes.

Gold nanoparticle synthesis

To 95 mL of 1 mM gold(III) chloride trihydrate solution, 5 mL of *C. halicacabum* aqueous extract was added and kept at room temperature for 15 minutes for the synthesis of *C. halicacabum*-gold nanoparticles (CH-AuNP). The color change of solution to ruby red from yellow signifies the synthesis of CH-AuNP,[18] and it was further confirmed by the characterization analysis using various techniques.

CH-AuNP characterization

UV-spectroscopy

The bioreduction property of CH-AuNP synthesized was assessed by using UV-Visible Spectrophotometer at a spectra range of 300–700 nm.

Selected area diffraction (SAED) analysis

The SAED pattern of the synthesized CH-AuNP was analyzed to determine the structure crystallinity by using Malvern Zetasizer instrument. The samples for SAED

analysis were prepared with Millipore filtered water to avoid possible contaminant reaction. The distance between the planes was calculated based on the patterns obtained after the SAED analysis.

Dynamic light scattering (DLS) analysis

The size and dispersal nature of the gold nanoparticles were determined by DLS particle size analyzer IG-1000 plus (Shimadzu, Japan). Sample was mixed with water and sonicated for 20 minutes and assessed.

Fourier-transform infrared (FTIR) spectroscopy analysis

FTIR spectroscopy analysis was performed to identify the functional groups present in the biosynthesized CH-AuNP. The dried powder of CH-AuNP weighing 2 mg was mixed with 200 mg of potassium bromide and placed in the sample holder. This mixture was subjected to FTIR spectroscopy analysis at a range of 4,000–500 cm^{-1} spectra using FTIR Spectrum 2,000, Perkin Elmer (Waltham, MA, USA). About 50 scans at a resolution of 4 cm per scan were performed and the data obtained were assessed using the software WINFIRST (Mattson, Madison, WI, USA).

Atomic force microscopy (AFM) analysis

The size of the CH-AuNP synthesized was measured using AFM analysis. The synthesized nanoparticles were placed on a silica probe and dried with nitrogen gas, and then analyzed with contact mode of Perkin Elmer atomic force microscope.

Transmission electron microscopy-electron diffraction X (TEM-EDX) analysis

The size, morphology, and the composition CH-AuNP synthesized were assessed by using high-resolution transmission electron microscope. The presence of gold element in the CH-AuNP synthesized was confirmed by subjecting the sample to TEM-EDX analysis. The CH-AuNP sample was mixed with methanol by subjecting to ultrasonication and then placed on the carbon film and assessed for EDX analysis in JEOL instrument by subjecting it to 200 kV voltage.

Cytotoxic effect of CH-AuNP on gastric carcinoma cell lines

Culturing of gastric carcinoma cell lines

Human gastric carcinoma cell lines AGS, SNU-5, and SNU-16 were obtained from Institute of Biochemistry and Cell Biology, Chinese Academy of Sciences (Shanghai, China). RPMI 1640 medium (Thermo Fisher Scientific, Waltham, MA, USA) was used for culturing all the three types of cells, the cells were supplemented with FBS (10%) (Thermo Fisher Scientific), and 1% antibiotic–antimycotic solution was added to avoid contamination. The cells were incubated at 37°C with 5% CO_2, and the medium was replaced every 48 hours. The cells were trypsinized for subculturing when it reached 80% confluency with 0.25% trypsin and 0.02% EDTA.

Cytotoxicity assay

The cytotoxicity of biosynthesized CH-AuNP against various gastric carcinoma cell lines was assessed by MTT assay.[19] The destruction of cell mitochondria was assessed by estimating the formation of blue formazan crystals, which were formed by reduction of MTT by mitochondrial succinic dehydrogenase secreted by viable cells. In each well (200 µL $well^{-1}$) of 96-well microtiter plates, 10^5 numbers of cells were plated, and they were incubated with different concentrations of CH-AuNPs ranging from 0 to 50 µg/mL at 37°C in a CO_2 incubator for 24 hours. After 24 hours, the cell viability was measured by MTT assay, and the CH-AuNP's CC50 was calculated, which is used for analysis of anticancer activity.

Apoptotic cell morphology analysis

DAPI staining

The anticancer effect of CH-AuNPs was assessed by analyzing the morphology of cells exposed to various concentrations of CH-AuNPs using DAPI stain and TUNEL assay. In six-well plates, 2×10^5 cells were inoculated, and they were incubated with 25 and 50 µg/mL of CH-AuNP at 37°C for 24 hours with 5% CO_2. After 24-hour incubation, the cells were fixed with glutaraldehyde 2.5% and Triton X-100 0.1% for 15 minutes. Then the cells were stained with DAPI stain for 5 minutes at a temperature of 37°C, and the cells were then washed with PBS and viewed in NIKON Eclipse 80i fluorescent microscope (Nikon Corporation, Tokyo, Japan).

TUNEL assay

The TUNEL assay was done using the TUNEL assay kit obtained from Abcam (USA). Using 1% paraformaldehyde, the cells were fixed for 15 minutes, and after fixation the cells were rinsed with PBS. Then the cells were treated with 70% ethanol and incubated for 30 minutes on ice, and after incubation the cells were washed with buffer and 50 µL of DNA labeling solution was added to the cells, and incubated for 1 hour at 37°C. The cells were then washed with buffer after incubation and suspended again in propidium iodide (PI)

solution for 30 minutes and incubated at dark. The cells were then observed under NIKON Eclipse 80i fluorescent microscope (Japan).

Acridine orange (AO)/PI dual staining

Double staining of cells with AO and PI clearly indicates the difference between dead and live cells. AO stains all the cells irrespective of being dead or alive, whereas the PI stains only the dead cells. The cells exposed to CH-AuNP were fixed with 0.1% Triton X-100 and then stained with 10 µL of AO (1 mg/mL) and PI (2.5 mg/mL). The cells were incubated for 15 minutes at dark and then viewed under fluorescent microscope; the cells that fluoresce in green color are alive cells and the red fluorescence cells are dead cells.

Flow cytometry analysis

AGS cells were seeded in six-well plates and then treated with various concentrations of CH-AuNP for 24 h. The cells were harvested and stained with Annexin V-fluorescein isothiocyanate and PI for 15 minutes at room temperature. Samples were analyzed by flow cytometer (FACSCalibur, BD, San Jose, CA, USA) and CELLQuest software (FACSCalibur).

Mitochondrial membrane potential (MMP) determination

The MMP was measured with JC-1 Mitochondrial Membrane Potential Detection kit based on the manufacturer's instructions. AGS cells were treated with various concentrations of CH-AuNP for 24 h. Collected cells were incubated with JC-1 for 20 min at 37°C. The stained cells were washed twice and analyzed by a flow cytometer. The MMP was recorded using a flow cytometer equipped with CellQuest software (BD Biosciences).

Caspases activity

The activity of proteases caspases was detected using the caspase-3 (ab39401) and caspase-9 (ab65608) kits purchased from Abcam (Cambridge, UK). caspases 3 and 9 recognize the sequence DEVD and LEHD, respectively, and cleave from the labeled substrate p-NA emitting light, which was quantified using a spectrophotometer at 405 nm.

ROS analysis

The ROS generated by the CH-AuNP were evaluated by using the kit H2DCFDA (Thermo Fisher Scientific). The fluorescence of 2′, 7′-dichlorodihydrofluorescein diacetate acetyl ester produced by the reduction of DCFDA due to cellular oxidation was estimated to detect and quantify the oxidative stress created.[19] The most sensitive AGS gastric carcinoma cell lines were exposed to 25 and 50 µg concentration for 24 hours. After incubation, the cells were washed with buffered saline and then incubated to 80 mM H2DCFDA for 30 minutes at 37°C. The intensity of the fluorescence exhibited was measured at 530 nm and the values were normalized with the concentration of protein.

Antiapoptotic effect of CH-AuNP gastric carcinoma cell line

Immunoblotting analysis

The expression of the apoptotic protein after the exposure of different concentrations of CH-AuNP on gastric carcinoma AGS cells was assessed by immunoblotting analysis. The control and CH-AuNP-treated cells were washed with PBS and lysed by sonicating using 200 µL of ice-cold lysis buffer. The sonicated cells were then subjected to centrifugation for 30 minutes at 4°C, 10,000 × *g*. The supernatant was collected and quantified for protein using Bradford reagent. Fifty micrograms of protein from each group were mixed with sample buffer, boiled for 5 minutes at the temperature of 95°C, and subjected to electrophoresis with 10% SDS-PAGE. The electrophoresed sample was then transferred to a polyvinylidene difluoride membrane blocked with 5% skimmed milk for 1 hour and the membrane was incubated with mouse monoclonal anti-human Bcl-2 (sc-7382), Bcl-xl (sc-8392), Bax (sc-7480), caspase-3 (sc-7272), caspase-9 (sc-56073), and β-actin (sc-47778) antibodies for 12 hours. The secondary anti-mouse horseradish peroxidase-labeled antibodies were added to the membrane after a wash with PBS. The bands of the protein were then viewed using ECL kit, Perkin Elmer, USA.

Statistical analysis

The data were expressed as mean ± SD of three independent observations. Data were subjected to statistical analysis by performing one-way ANOVA followed by Student–Newman–Keul's test using Graph Pad Prism 4 statistical software. The *P*-values <0.01 were considered significant.

Results

Characterization of CH-AuNP

UV-visible spectroscopic and DLS analysis

The biosynthesis of gold nanoparticles with *C. halicacabum* was confirmed with UV-visible spectroscopic analysis. Due to the surface plasmon resonance excitation property of the synthesized gold nanoparticles, maximum absorbance peak

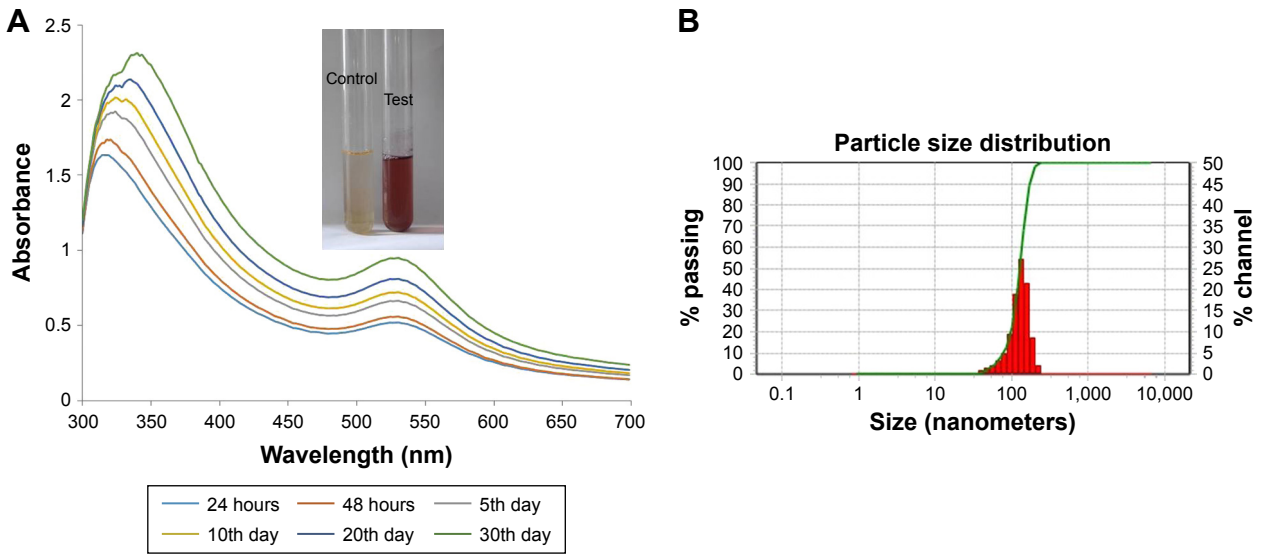

Figure 1 UV-visible spectrum absorption pattern and DLS of Ch-AuNP.
Notes: (**A**) UV-visible spectrum of synthesized Ch-AuNP; (**B**) DLS analysis.
Abbreviations: Ch-AuNP, *C. halicacabum*-gold nanoparticles; DLS, dynamic light scattering.

was observed at 350 and 525 nm with the formation of violet color. The sample was analyzed at different time intervals of 24 hours, 48 hours, 5 days, 10 days, 20 days, and 30 days (Figure 1A), and the maximum peak was observed for the 30th-day sample, indicating that as the time increases the amount of conversion of gold nanoparticle also increases. The size of the nanoparticle synthesized is measured with DLS analysis and the size distribution curve is depicted in Figure 1B. The particle size ranged from 35.1 to 150.1 nm and had an average particle size of 128 nm with a polydispersity index value of 0.912.

FTIR spectroscopy analysis

The FTIR spectrum of the synthesized CH-AuNPs is shown in Figure 2A. The maximum peak range of CH-AuNPs was seen between 1,500 and 3,500 cm^{-1}, with characteristic peaks at 1,367 (C–H rock), 2,117 (C=O), and 3,313 cm^{-1} (O–H stretch or H bond), which is due to the reduction of

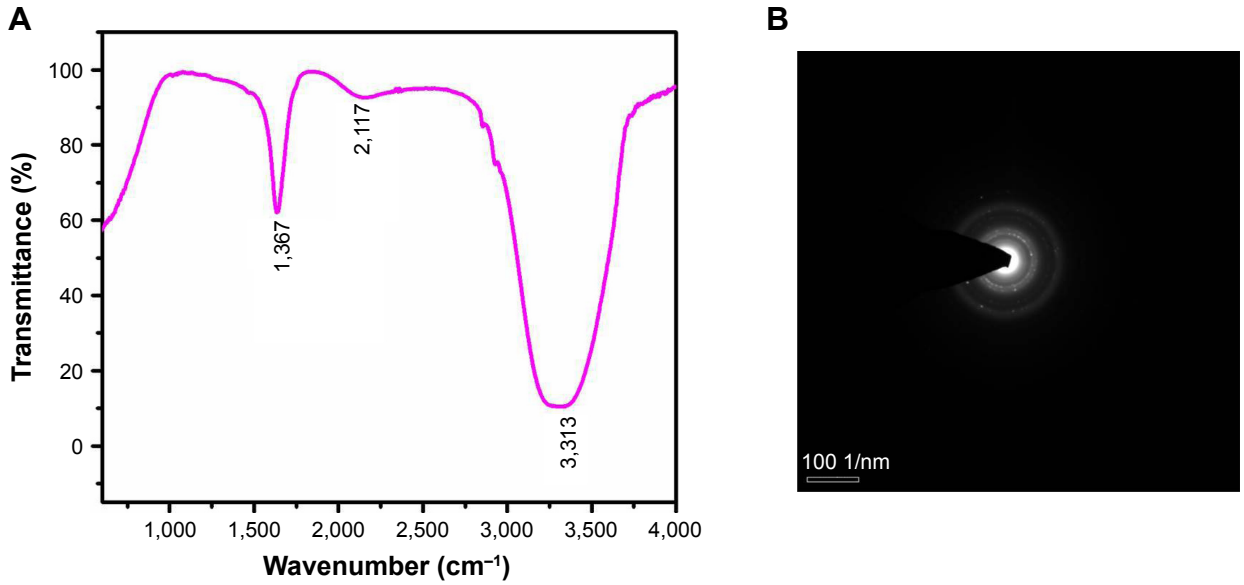

Figure 2 FTIR spectroscopy analysis and SAED pattern of gold nanoparticles synthesized from *Cardiospermum halicacabum*.
Notes: (**A**) FTIR spectroscopy analysis; (**B**) SAED pattern.
Abbreviations: SAED, selected area diffraction; FTIR, Fourier-transform infrared.

gold ions by *C. halicacabum*. The peak at 3,313 cm^{-1} indicates the presence of hydroxyl group of polyphenols from *C. halicacabum*, and the stretch at 2,117 cm^{-1} specifies the presence of aldehydes, esters, and ketones.

Morphological characterization of CH-AuNP

Figure 2B shows the SAED pattern of gold nanoparticles biosynthesized from *C. halicacabum*, and the nanoparticles exhibit ring-like structure, which indicates the crystalline nature of the nanoparticles. The high-resolution transmission electron microscopy analysis of CH-AuNP is depicted in Figure 3A, which shows that they are of spherical shape and that they are polydispersed at an average diameter of 30.05 nm. EDAX analysis confirmed the presence of gold particles by exhibiting characteristic peak and it also exhibited weak copper peak, which may be due to the presence of other molecules bound to the surface of AuNP (Figure 3B).

AFM analysis

The topographical structure of biosynthesized CH-AuNPs was analyzed by AFM (Figure 4). The AFM analysis confirmed the nanosphere shapes of the gold nanoparticles, which correlates with the TEM image.

Anticancer activity of CH-AuNP

IC_{50} dose analysis of CH-AuNP

The IC_{50} dose of synthesized CH-AuNP was analyzed by performing MTT assay (Figure 5). Three different gastric carcinoma cell lines AGS, SNU-5, and SNU-16 were treated with eight different concentrations of CH-AuNP ranging from 0 to 100 µg/mol for 24 hours and subjected to MTT analysis. AGS cell lines were more sensitive to CH-AuNP compared to SNU-5 and SNU-16, and about 50% of cells were dead in AGS cells treated with 25 µg/mol. Hence, for the further assessment of anticancer activity of CH-AuNP in the AGS gastric cell line, a dosage of 25 µg/mol was selected.

CH-AuNP apoptotic effect

Dual staining with AO and PI was done to detect the apoptotic cells induced by the CH-AuNPs, which was further confirmed with TUNEL assay and DAPI staining (Figure 6A). Increased red fluorescence was observed in the cells treated with 50 µg/mol of CH-AuNP stained with dual stain. DAPI staining and TUNEL assay also confirm the apoptotic effect of CH-AuNP on AGS cell line. The flow cytometry analysis has shown that CH-AuNP-treated AGS cells induce the apoptosis in a time-dependent manner. CH-AuNP (25 µg)

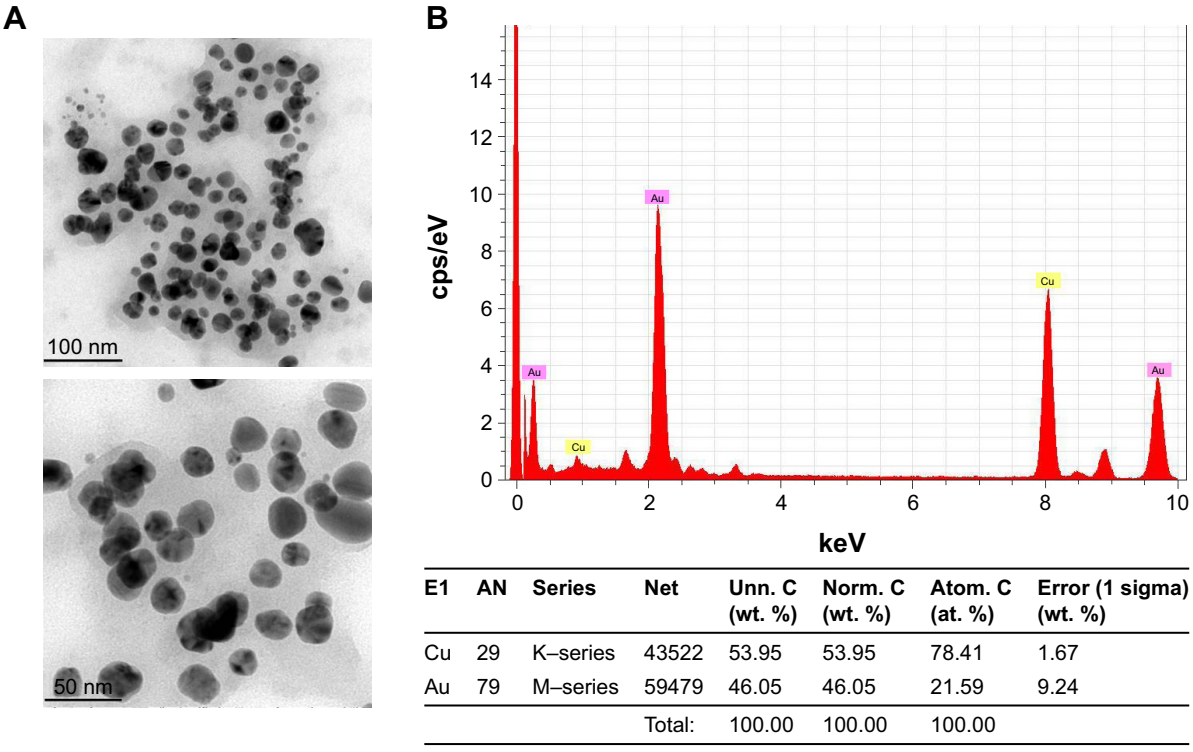

E1	AN	Series	Net	Unn. C (wt. %)	Norm. C (wt. %)	Atom. C (at. %)	Error (1 sigma) (wt. %)
Cu	29	K–series	43522	53.95	53.95	78.41	1.67
Au	79	M–series	59479	46.05	46.05	21.59	9.24
			Total:	100.00	100.00	100.00	

Figure 3 HR-TEM and energy-dispersive X-ray analysis of Ch-AuNP.
Notes: (**A**) HR-TEM images of Ch-AuNP; (**B**) energy-dispersive X-ray analysis of Ch-AuNP.
Abbreviations: Ch-AuNP, *Cardiospermum halicacabum*-gold nanoparticles; HR-TEM, high-resolution transmission electron microscopy.

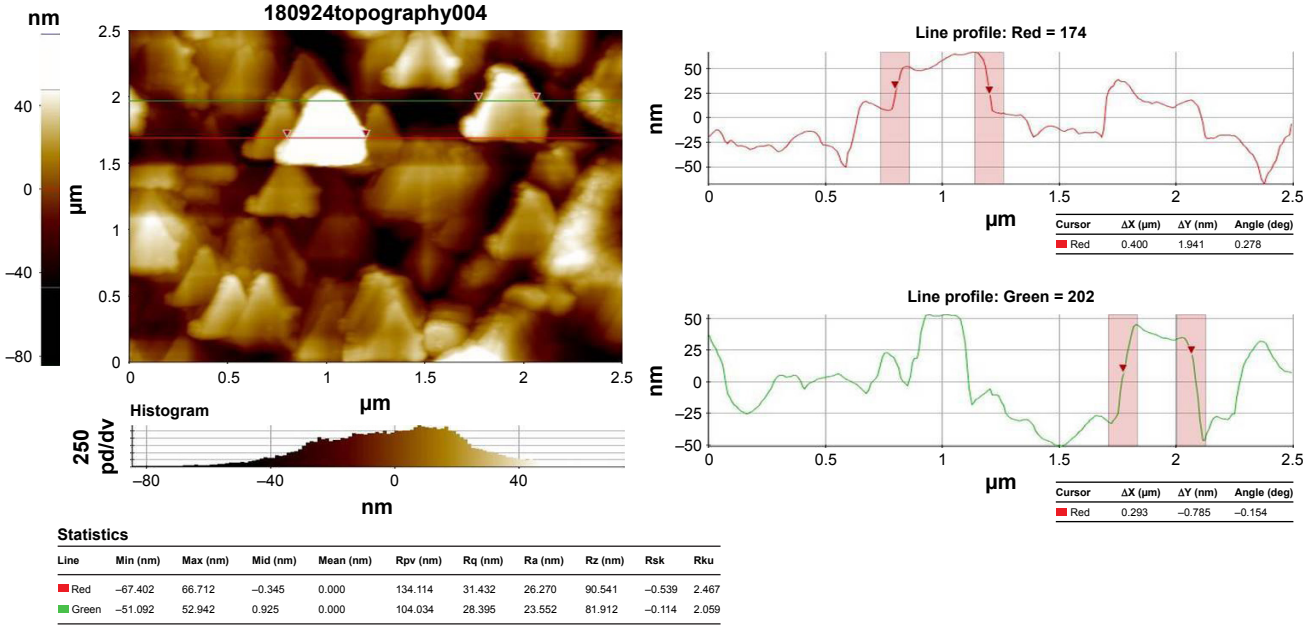

Figure 4 Atomic force microscopy analysis of gold nanoparticles synthesized from *Cardiospermum halicacabum*.

treatment showed the significant number of apoptotic cells (92.5%) in 24 hours (Figure 6B).

MMP

Figure 7 shows the analysis of MMP in AGS cells that were incubated with different concentrations of CH-AuNP. Following 25 and 50 µg/mL CH-AuNP treatment, AGS cells have explored a significantly minimum expression of JC-1 in mitochondria with the concentration of CH-AuNP compared to control cells.

Effect of CH-AuNP on caspases

Caspases are the cysteine-aspartate proteases that play an important role in apoptosis. Caspase-3 is the initiator caspase and caspase-9 is the executor caspase. Both the initiator and the executor caspases were increased in AGS gastric carcinoma cell lines treated with 25 and 50 µg/mol of CH-AuNP (Figure 8A and B).

Intracellular oxidative status of CH-AuNP treatment

The intracellular ROS content of control and CH-AuNP-treated AGS gastric carcinoma cells is depicted in Figure 8C.

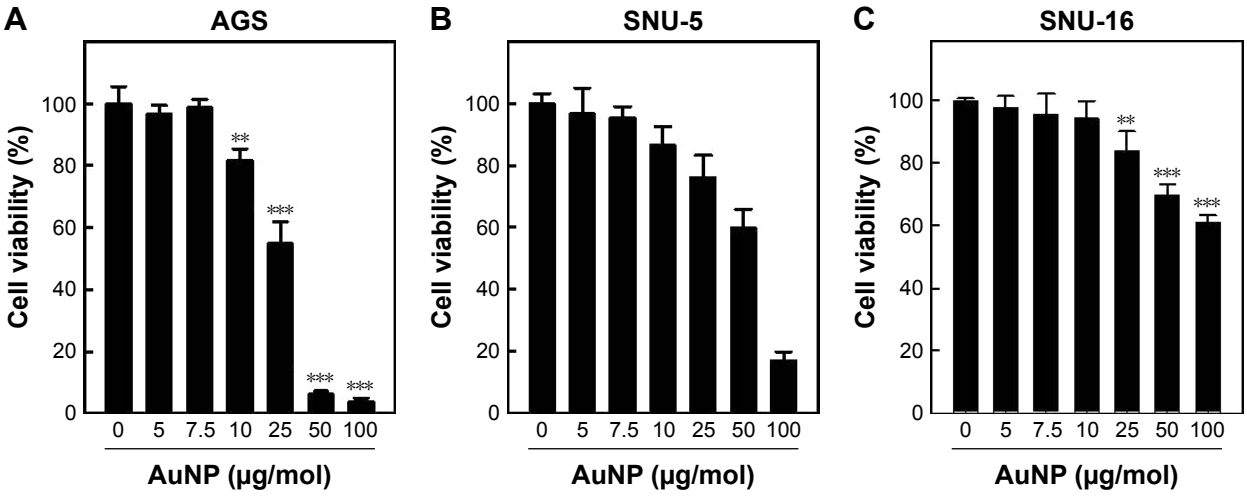

Figure 5 Cytotoxicity effect of Ch-AuNP.
Notes: (**A**–**C**) The normal human gastric cancer cells (AGS, SNU-5, SNU-16) were exposed to different concentrations of Ch-AuNP for 24 hours and the effect on cell viability was analyzed by MTT assay. The number of viable cells after treatment is expressed as a percentage of the vehicle-only control. This experiment was repeated thrice and the bars in the graph represent SE (**$P<0.05$, ***$P<0.01$).
Abbreviation: Ch-AuNP, *Cardiospermum halicacabum*-gold nanoparticles.

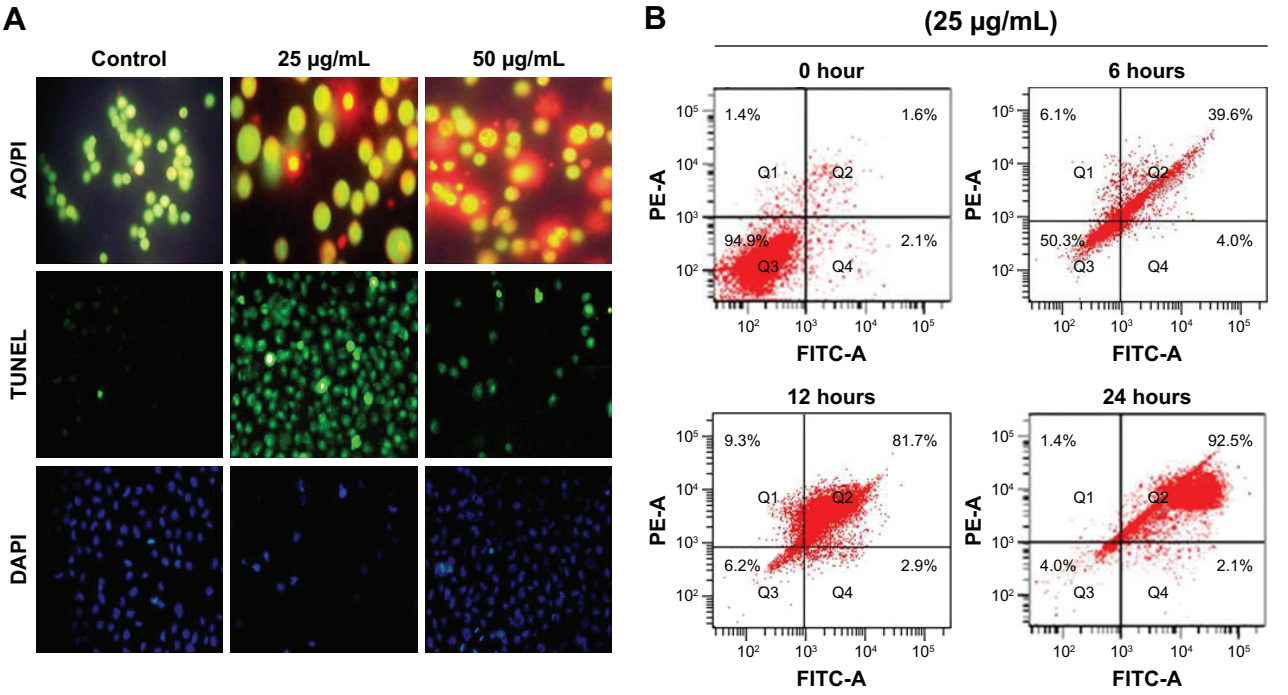

Figure 6 Apoptotic effect of gold nanoparticles synthesized from *Cardiospermum halicacabum* in AGS gastric carcinoma cell lines.
Notes: (**A**) Double staining technique by PI/AO, TUNEL, and DAPI staining; (**B**) Annexin V/fluorescein isothiocyanate.
Abbreviations: AO, Acridine orange; PI, propidium iodide.

Twenty-five percent and 75% increase in ROS content were observed in 25 and 50 µg/mol CH-AuNP-treated cells, respectively, which indicates the initiation of apoptosis by the biosynthesized CH-AuNP.

Effect of CH-AuNP on apoptotic signaling

Apoptosis is the programmed cell death carried out by the cells for the elimination of damaged cells, and the inhibition of apoptosis is the hallmark event of tumor initiation.

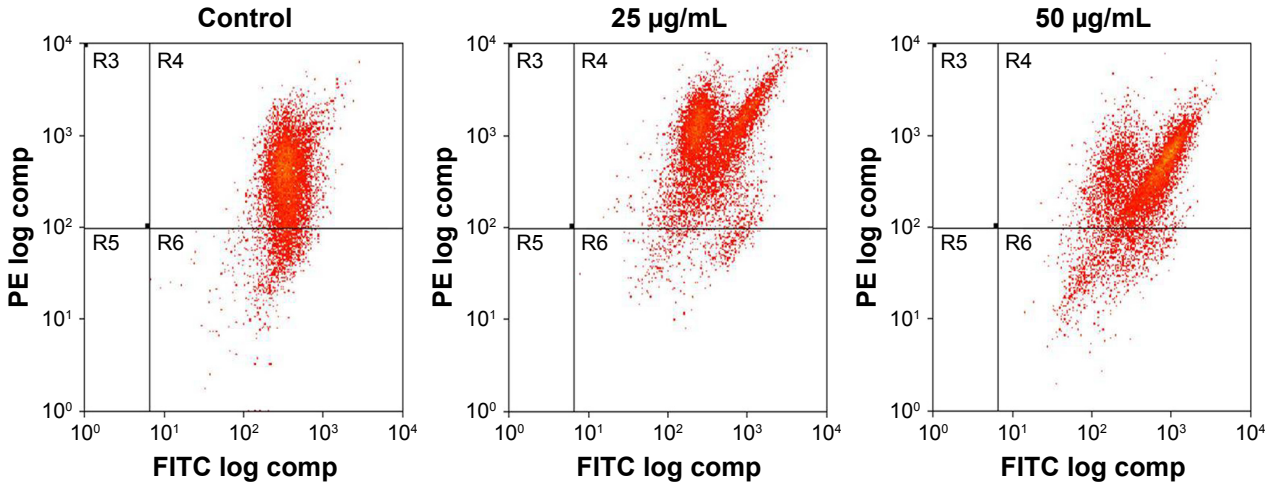

	Control	Ch-AuNP	
	Untreated	25 µg/mL	50 µg/mL
R4	96.40	94.90	85.22
R6	3.6	5.10	14.78

Figure 7 MMP disruption in AGS cells treated by Ch-AuNP for 24 hours.
Notes: MMP disruption in AGS cells treated by Ch-AuNP with various concentrations for 24 hours. The cells were stained with JC-1, and changes in the fluorescence were analyzed by flow cytometry. Density plots of FSC vs SSC showing the analysis gates R4 and R6 surrounding viable cells and apoptotic cells, respectively.
Abbreviations: Ch-AuNP, *Cardiospermum halicacabum*-gold nanoparticles; FITC, fluorescein isothiocyanate; MMP, mitochondrial membrane potential; FSC, forward scatter; SSC, side-scattered.

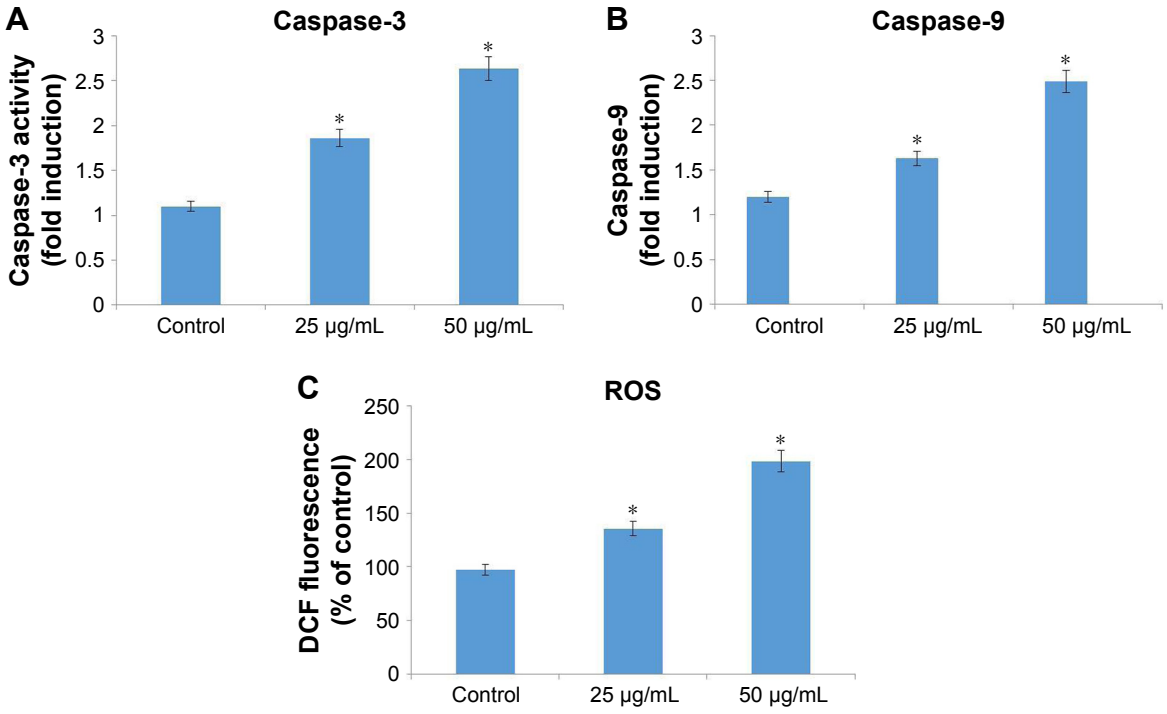

Figure 8 Effect of gold nanoparticles synthesized from *Cardiospermum halicacabum* on caspases (**A** and **B**) and ROS production (**C**) in AGS gastric carcinoma cell line.
Notes: Each bar represents mean ± SEM of three independent observations. *$P<0.05$ is considered as statistically significant.

Figure 9 exemplifies the levels of apoptotic protein expression in control and CH-AuNP-treated gastric carcinoma AGS cell lines. Compared to control, there is a marked increase in the expression of proapoptotic proteins Bax, and caspases 3 and 9, whereas the expression of antiapoptotic proteins Bcl-xl and Bcl-2 was decreased, indicating the initiation of apoptosis in cancer cells by the CH-AuNP.

Discussion

Cancer, which tends to be the second leading causative agent of mortality worldwide, is of global concern. In China, about 2.5 million people were estimated to be diagnosed with cancer, of which about 2 lakh deaths were reported to be due to poor diagnosis and treatment.[20] Among various types of cancers, gastric cancers tend to be the fourth common type of cancer leading to second cause of cancer-related deaths. Compared to developed countries the incidence and mortality of gastric cancer are more in developing countries. Highest incidence was reported in Eastern Asia, South America, and Central Europe.[21] Gastric cancer patients are treated with chemotherapy as the first choice of treatment, but it leads to serious side effects and the survival rate was also not increased in most cases.[22] Hence, alternative medicine is the need of today to treat cancer, and phytomedicine is once such field that shows promising evidence to treat cancer with less or nil side effects compared to conventional treatment.[23]

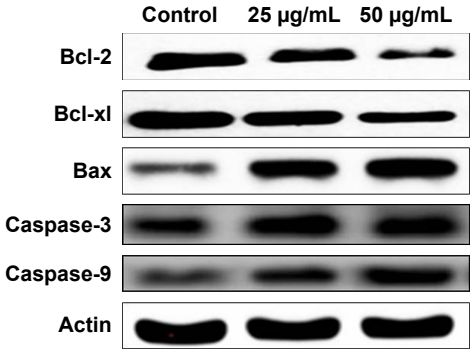

Figure 9 Anticancer effect of Ch-AuNP on apoptotic signaling proteins in AGS gastric carcinoma cell line.
Notes: AGS cells were treated with Ch-AuNP (25 and 50 µg) for 24 hours, and dose-dependent changes in the expressions of Bcl-2, Bax, Bcl-xl, and caspase-3 were monitored by Western blotting. β-actin was used as a loading control.
Abbreviation: Ch-AuNP, *Cardiospermum halicacabum*-gold nanoparticles.

C. halicacabum is a traditional medicine but now in modern era it is considered as a weed plant. It has been used to treat various diseases like nerve disorders, stiffness, rheumatism, and snakebite.[24] Recently, it was reported that the methanolic extract of *C. halicacabum* induced apoptosis in breast cancer cell line. In the present study, we biosynthesized gold nanoparticles with *C. halicacabum* and analyzed the efficacy against gastric carcinoma cell lines.

Gold nanoparticles possess exclusive physiochemical properties like surface plasmon resonance and binding capacity with amine and thiol groups, which makes it a

potent candidate in the biomedical field.[25] In the present study, we synthesized and characterized gold nanoparticles with *C. halicacabum*; gold nanoparticles were synthesized by reducing gold chloride with aqueous extract of *C. halicacabum*, and the red coloration confirms the synthesis of gold nanoparticles.[26] The red coloration is due to exclusive surface resonance property of gold, which is observed near 530 nm and it also indicates the uniform distribution of gold nanoparticles in the aqueous solution.[27,28]

The optical and electronic properties of gold nanoparticles depend on the shape of the nanoparticles.[29] TEM observation, which was done to analyze the shape of *C. halicacabum* biosynthesized gold nanoparticles, identified them to be spherical shaped. The composition of atoms present in CH-AuNPs was assessed by EDAX using TEM images. The EDAX analysis showed the presence of gold particles, which confirmed the formation of gold nanoparticles. The reduction of Au(III) to Au(0) was assessed by FTIR spectroscopy analysis, and the characteristic peaks at 1,367, 2,117, and 3,313 cm^{-1} indicate the reduction of gold, which may be due to the polyphenols that bind the gold metal with carbonyl group and caps the gold nanoparticle thus preventing from aggregation of nanoparticles. Gold nanoparticles are synthesized by binding of negatively charged $AuCl_4$ with positively charged ions.[30] In the present study, the active components of *C. halicacabum* could have bound to $AuCl_4$ and reduced it to gold nanoparticles.

Gold nanoparticles possess the property to inhibit the overexpression of signaling proteins like Ras and Akt in tumor cells; therefore, it can be used as an anticancer drug. In the current study, we analyzed the anticancer activity of gold nanoparticles synthesized with *C. halicacabum*. Mata et al[31] reported that when the gold nanoparticles of dosage 1.4 nm were used to treat the HeLa cell line it increased the oxidative stress, leading to mitochondrial impairment and apoptosis. The anticancer effect of CH-AuNP was analyzed with three different gastric carcinoma cell lines AGS, SNU-5, and SNU-16. CH-AuNP was more sensitive to AGS cell line and the IC_{50} dose was obtained at 25 µg/mL concentration. Selim and Hendi[32] reported that when the gold nanoparticles of dosage 1.4 nm were used to treat the HeLa cell line, it increased the oxidative stress leading to mitochondrial impairment and apoptosis. The same results were obtained in the present study, which is documented with AO/PI, DAPI, and TUNEL assay.

The MMP plays a vital role in triggering mitochondria-mediated apoptosis by the activation of caspase-9 and the translocation of Bax.[33] In the present study, CH-AuNP treatment induced mitochondria-mediated apoptosis in AGS cells by reactivity with the fluorescent dye, JC-1, that enters the mitochondrial matrix and stains the mitochondria of healthy cells red due to formation of J-aggregates.

Programmed cell death or apoptosis is the critical process that prevents the progression of cancer.[34] Apoptosis is initiated and executed by various proteins, and B-cell lymphoma 2 family proteins are the key proteins that balance the survival and death of the cells. Bcl group of proteins consist of both proapoptotic proteins that induce apoptosis and antiapoptotic proteins that inhibit apoptosis.[35] In the current study, we examined the effect of biosynthesized CH-AuNP on Bcl group of proteins. CH-AuNP increased the expression of proapoptotic protein Bax and inhibited the expression of antiapoptotic protein Bcl-2 and Bcl-xl. It also increased the protein expressions of both caspases, the initiator caspase-3 and executor caspase-9. Caspases are vital proteins that induce carcinogenesis, neurodegeneration, immunodeficiency, and autoimmunity.[36] The increase in caspases may be due to the anticancer property of CH-AuNP, which increased the intracellular ROS production thereby inducing apoptosis. Gold nanoparticles are promising nanocarriers because of their easy synthesis and the biocompatibility, and this also would have increased the anticancer property of *C. halicacabum*.

The DAPI staining of AGS cell line treated with CH-AuNP clearly indicates the induction of apoptosis by CH-AuNP. The cells treated with CH-AuNP showed condensed nucleus along with the loss in cell structure. It is further confirmed with the increased red fluorescence exhibited by CH-AuNP-treated cells when stained with AO/PI. The red fluorescence is due to the uptake of AO by the dead cells, whereas the live cell emits green fluorescence. The overall staining results confirm the induction of apoptosis by CH-AuNP by the presence of condensed nucleus and shrunken nucleus, which are the hallmarks of apoptotic cells. It was also confirmed with the increased caspases and increased expression of proapoptotic proteins, which indicates that the synthesized CH-AuNP is a potent anticancer drug.

Conclusion

To conclude, in the present study, we biosynthesized gold nanoparticles using extract of *C. halicacabum* using a simple, cost-effective method. The spectroscopical and morphometric analysis confirms the synthesis of nanospheric gold nanoparticles with an average diameter of 30.5 nm. The anticancer activity of CH-AuNPs was analyzed in vitro with gastric carcinoma cell lines, and it is confirmed that they effectively induce apoptosis via inhibiting antiapoptotic proteins and inducing proapoptotic proteins in the AGS cell

line at an IC_{50} value of 25 μg/mL. Hence, it evident that CH-AuNP is a potent anticancer drug in vitro, and further research in vivo can be done to formulate CH-AuNPs as a cost-effective anticancer drug.

Disclosure

The authors report no conflicts of interest in this work.

References

1. Ferlay J, Shin HR, Bray F, Forman D, Mathers C, Parkin DM. Estimates of worldwide burden of cancer in 2008: GLOBOCAN 2008. *Int J Cancer*. 2010;127(12):2893–2917.
2. Zhu AL, Sonnenberg A. Is gastric cancer again rising? *J Clin Gastroenterol*. 2012;46(9):804–806.
3. Kodera Y. Treatment strategy for liver metastasis from gastric cancer. *Nih on Geka Gakkai Zasshi*. 2012;113(1):22–25.
4. Lahmidani N, El Yousf M, Aqodad N, et al. Update on gastric cancer epidemiology and risk factors. *J Cancer Ther*. 2018;9(3):242–254.
5. Yamamoto T, Mori T, Sawada M, et al. Loss of AF-6/afadin induces cell invasion, suppresses the formation of glandular structures and might be a predictive marker of resistance to chemotherapy in endometrial cancer. *BMC Cancer*. 2015;15(1):275.
6. Fu Y, Du P, Zhao J, Hu C, Qin Y, Huang G. Gastric cancer stem cells: mechanisms and therapeutic approaches. *Yonsei Med J*. 2018;59(10):1150–1158.
7. Koizumi M, Saga T, Yoshikawa K, Baba M. Gastric cancer found on 3′-deoxy-3′ F-18 fluorothymidine positron emission tomography. *Clin Nucl Med*. 2008;33(9):641–642.
8. Shekhawat MS, Manokari M, Kannan N, Pragasam A. In vitro clonal propagation of *Cardiospermum halicacabum* L. through nodal segment cultures. *Pharma Innovation*. 2012;1(7):1–7.
9. Nadkarni KM. *The Indian Materia Medica, with Ayurvedic, Unani and Home Remedies.* Revised and enlarged by Natkarni AK, editor. 1954, 3rd ed. Bombay, India: Bombay Popular Prakashan PVP; 1976:271–272.
10. Chopra RN, Nayar SLR, Chopra IC. *Glossary of Indian Medicinal Plants*. New Delhi: Council of Scientific and Industrial Research; 1986.
11. Iwu MW, Duncan AR, Okunji CO. New antimicrobials of plant origin. In: Janick J, editor. *Perspectives on New Crops and New Uses*. Alexandria, VA: ASHS Press; 1993:457–462.
12. Chung TH, Kim JC, Kim MK, et al. Investigation of Korean plant extracts for potential phytotherapeutic agents against B-virus hepatitis. *Phytotherapy Res*. 1995;9(6):429–434.
13. Aaseth J, Haugen M, Førre O. Rheumatoid arthritis and metal compounds – perspectives on the role of oxygen radical detoxification. *Analyst*. 1998;123(1):3–6.
14. Patra CR, Bhattacharya R, Mukhopadhyay D, Mukherjee P. Fabrication of gold nanoparticles for targeted therapy in pancreatic cancer. *Adv Drug Deliv Rev*. 2010;62(3):346–361.
15. Lewinski N, Colvin V, Drezek R. Cytotoxicity of nanoparticles. *Small*. 2008;4(1):26–49.
16. Jain KK. The role of nanobiotechnology in drug discovery. *Adv Exp Med Biol*. 2009;655:37–43.
17. Karuppaiya P, Satheeshkumar E, Chao W-T, Kao L-Y, Chen EC-F, Tsay H-S. Anti-metastatic activity of biologically synthesized gold nanoparticles on human fibrosarcoma cell line HT-1080. *Colloids Surf B Biointerfaces*. 2013;110:163–170.
18. Sindhu K, Rajaram A, Sreeram KJ, Rajaram R. Curcumin conjugated gold nanoparticle synthesis and its biocompatibility. *RSC Adv*. 2014;4(4):1–11.
19. Mosmann T. Rapid colorimetric assay for cellular growth and survival: application to proliferation and cytotoxicity assays. *J Immunol Methods*. 1983;65(1–2):55–63.
20. Oyama Y, Hayashi A, Ueha T, Maekawa K. Characterization of 2′,7′-dichlorofluorescin fluorescence in dissociated mammalian brain neurons: estimation on intracellular content of hydrogen peroxide. *Brain Res*. 1994;635(1–2):113–117.
21. Ibrahim M, Gilbert K. Management of gastric cancer in Indian population. *Transl Gastroenterol Hepatol*. 2017;2(8):64.
22. Nagaich N, Sharma R. Gastric cancer – an update. *J Tumor Med Prev*. 2018;2:5.
23. Yamamoto H, Gotoda T, Nakamura T, et al. Clinical impact of gastroenterologist-administered propofol during esophagogastroduodenoscopy: a randomized comparison at a single medical clinic. *Gastric Cancer*. 2015;18(2):326–331.
24. Chaudhary P, Gupta S, Leekha N, Tandon R, Nandy M, De S. Pattern of occurrence and treatment outcome of second primary malignancies: a single center experience. *South Asian J Cancer*. 2017;6(3):137–138.
25. Joshi SK, Sharma BD, Bhatia CR, Singh RV, Thakur RS. *The Wealth of Indian Raw Materials*. New Delhi, India: CSIR Publication; 1992.
26. Chanda N, Shukla R, Katti KV, Kannan R. Gastrin releasing protein receptor specific gold nanorods: breast and prostate tumor avid nanovectors for molecular imaging. *Nano Lett*. 2009;9(5):1798–1805.
27. Link S, El-Sayed MA. Shape and size dependence of radiative, nonradiative and photothermal properties of gold nanocrystals. *Int Rev Phys Chem*. 2000;19(3):409–453.
28. Rajathi FA, Parthiban C, Kumar VG, Anantharaman P. Biosynthesis of antibacterial gold nanoparticles using brown alga, *Stoechospermum marginatum* (kützing). *Spectrochim Acta A Mol Biomol Spectrosc*. 2012;99:166–173.
29. Chandran SP, Chaudhary M, Pasricha R, Ahmad A, Sastry M. Synthesis of gold nanotriangles and silver nanoparticles using *Aloe vera* plant extract. *Biotechnol Prog*. 2006;22(2):577–583.
30. Srivastava SK, Yamada R, Ogino C, Kondo A. Biogenic synthesis and characterization of gold nanoparticles by *Escherichia coli* K12 and its heterogeneous catalysis in degradation of 4-nitrophenol. *Nanoscale Res Lett*. 2013;8(1):70.
31. Mata R, Nakkala JR, Sadras SR. Polyphenol stabilized colloidal gold nanoparticles from *Abutilon indicum* leaf extract induce apoptosis in HT-29 colon cancer cells. *Colloids Surf B Biointerfaces*. 2016;143:499–510.
32. Selim ME, Hendi AA. Gold nanoparticles induce apoptosis in MCF-7 human breast cancer cells. *Asian Pac J Cancer Prev*. 2012;13(4):1617–1620.
33. Li HY, Zhang J, Sun LL, et al. Celastrol induces apoptosis and autophagy via the ROS/JNK signaling pathway in human osteosarcoma cells: an in vitro and in vivo study. *Cell Death Dis*. 2015;6(1):e1604.
34. Rengarajan T, Nandakumar N, Rajendran P, Haribabu L, Nishigaki I, Balasubramanian MP. D-pinitol promotes apoptosis in MCF-7 cells via induction of p53 and Bax and inhibition of Bcl-2 and NF-κB. *Asian Pac J Cancer Prev*. 2014;15(4):1757–1762.
35. Ashkenazi A, Fairbrother WJ, Leverson JD, Souers AJ. From basic apoptosis discoveries to advanced selective BCL-2 family inhibitors. *Nat Rev Drug Discov*. 2017;16(4):273–284.
36. Fathi N, Rashidi G, Khodadadi A, Shahi S, Sharifi S. STAT3 and apoptosis challenges in cancer. *Int J Biol Macromol*. 2018;117:993–1001.